Received 20 July 2021; revised 30 October 2021; accepted 8 November 2021. Date of publication 11 November 2021; date of current version 26 November 2021.

Digital Object Identifier 10.1109/OJAP.2021.3127312

A Foldable Reflectarray on a Hexagonal Twist Origami Structure

ANTONIO J. RUBIO[1] (Graduate Student Member, IEEE), ABDUL-SATTAR KADDOUR[1] (Member, IEEE), COLLIN YNCHAUSTI[2], SPENCER MAGLEBY[2], LARRY L. HOWELL[2], AND STAVROS V. GEORGAKOPOULOS[1] (Senior Member, IEEE)

[1]Department of Electrical and Computer Engineering, Florida International University, Miami, FL 33199 USA

[2]Department of Mechanical Engineering, Brigham Young University, Provo, UT 84602 USA

CORRESPONDING AUTHOR: A.-S. KADDOUR (e-mail: akaddour@fiu.edu)

This work was supported in part by the Air Force Office of Scientific Research under Grant FA9550-19-1-0290, and in part by the Utah NASA Space Grant Consortium.

ABSTRACT In this paper, a novel deployable flat panel reflectarray antenna (RA) is designed on an origami folding pattern for Small Satellite applications. The RA aperture deploys into a hexagonal geometry that achieves an aperture efficiency of a least 60%, 10-20% higher than current rectangular apertures. The modified hexagonal twist folding structure can achieve high volume packing efficiency, which is 75%, and simple deployment with one degree of freedom. The mechanical and electromagnetic design considerations for two variations of our proposed structure, flat and offset panels, are presented. The aperture surface area of both structures is $58\lambda^2$. Both structures are designed to operate at 16 GHz and exhibit a realized gain that is greater than 26.4 dBi. Prototypes are fabricated for the two structures and measured. Measurements show good correlation with the simulations.

INDEX TERMS Reflectarray antenna, origami, deployable, small satellite, aperture efficiency, packing efficiency.

I. INTRODUCTION

RECENT developments in small satellite (SmallSat) technology have enabled more efficient and robust space missions. These advancements have led to an exponentially increasing number of SmallSats being launched each year. At least 8,000 SmallSats are expected to be in lower earth orbit by the year 2024 to support the novel communications networks proposed by OneWeb, SpaceX, and Telesat alone [1], [2]. However, the reduced size of SmallSats presents significant challenges for engineers. Specifically, within the constraints of the SmallSat bus, it is very difficult to design communications systems that meet the requirements of space applications. Therefore, High Gain Antennas (HGAs), such as parabolic reflector antennas [3], phased array antennas [4], and Reflectarray Antennas (RAs) [5], have been proposed since they can transmit signals over longer distances. The increased energy efficiency of HGAs reduces the overall power requirements of space missions, thereby minimizing the size of power systems and creating more available space for other systems, while simultaneously reducing the mass of spacecraft. However, not all HGAs are suited for SmallSat applications. Despite their ultra-wideband operation and high gain features, traditional parabolic reflectors are bulky and have limited radiation versatility. Meanwhile, phased arrays, despite their low profile and versatile radiation capability, are also not ideal for SmallSats, since they require lossy and complex feeding networks. On the other hand, RAs combine the best features of parabolic reflectors and phased arrays and provide high gain, while maintaining low profile, low loss, and versatile radiation performance [6]. However, recently proposed deployable RAs used in SmallSat applications [6], [7] suffer from limited aperture efficiency, η_a (<50%), due to their rectangular apertures, which were used to achieve high packing efficiency.

In this paper, we propose a novel deployable and highly efficient flat-panel RA for SmallSat applications. The aperture of the proposed RA is designed on a novel modified

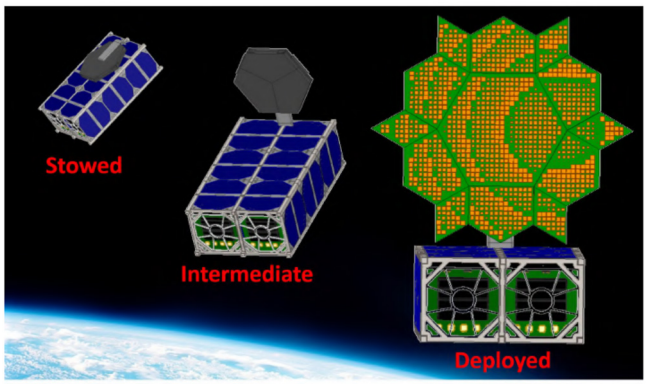

FIGURE 1. Proposed Hexagonal Twist reflectarray aperture on a 6U CubeSat.

hexagonal twist origami structure, which allows for simple deployment with one degree of freedom. Also, the aperture stows into a compact hexagonal shape, as seen in Fig. 1, thereby providing a high volume packing efficiency of 75%. In addition, the proposed origami folding pattern allows for membrane hinges to be used in the deployment mechanism, thereby eliminating the use of mechanical hinges on the reflecting surface of the aperture. At its deployed state, the proposed RA aperture has a hexagonal geometry, thus a 10-20% higher aperture efficiency than traditional deployable RAs with rectangular apertures. Specifically, our hexagonal aperture achieves at least 60% aperture efficiency, which enables our RA to achieve high gain (>26 dBi) with a miniaturized aperture surface area of $58\lambda^2$, where λ is the wavelength at the operating frequency (16 GHz). Two variations of the modified hexagonal twist aperture are presented. The first one is a flat structure in which the reflecting elements lie on a single plane, while the second one is an offset structure where the reflecting elements are distributed across two planes. The electromagnetic characteristics of both apertures are studied and compared to simulations. Initially, we presented a modified hexagonal twist RA aperture in [8], but it was not fully developed. The aperture was designed using the offset panel thickness accommodation method. Only an analytical study of the RA radiation pattern was performed using an ideal point source feed. In this work, we build upon the findings made in [8] by fully characterizing the offset aperture in terms of its electromagnetic and mechanical properties. Additionally, we present a flat version of the hexagonal origami RA aperture. Then, prototypes of the RA systems are fabricated and measured. Furthermore, studies on the effect of unit-cell size and panel offset are presented to give developers insight into possible methods for optimizing origami type RA apertures. The results of this work demonstrate that our proposed RAs are very well-suited for various SmallSat applications, such as, deep space and earth sciences.

The paper is organized as follows: Section II provides a brief summary of related works in the fields of origami and deployable RAs. Section III describes an analytical study of the aperture geometry and its effect on efficiency. The hexagonal twist origami patterns and their corresponding mechanical designs are presented in Section IV and Section V, respectively. Section VI describes the electromagnetic design considerations of our proposed RAs, as well as the fabrication of prototypes and their characterization through measurements. Finally, conclusions are drawn in Section VII.

II. RELATED WORKS

Many deployable HGA designs, including many deployable RA designs, have been proposed for SmallSat applications [9]–[12]. In [13], a deployable RA aperture was fabricated out of a polyimide membrane to achieve high gain (>50 dBi) and high packing efficiency using a 10U stowed volume. However, this design required a complicated system of trusses, lanyards and motors to deploy the aperture and maintain it under tension, which increases the costs, likelihood of failure, and mass of the spacecraft. Alternatively, inflatable RA systems have been proposed in [14] and [15] to achieve high gain with low mass, high packing efficiency, and simple deployment. However, these inflatable designs require compressed air to maintain the rigidity and flatness of the aperture which drastically decreases the life span of SmallSats. Finally, deployable folded flat-panel RAs (FPR) have been recently proposed [7], [16], and have been validated in deep space and low earth orbit missions. The advantage of such FPR designs is their use of rigid microstrip panels, which allow for low manufacturing cost, high packing efficiency, and simple deployment mechanisms. However, these FPR systems suffered from limited aperture efficiency (reported η_a of 42% and 26% in the MarCO [7] and ISARA [12] missions, respectively) due to their rectangular geometry and spring hinged deployment mechanisms. Improving the η_a of deployable FPRs would enable the reduction of the RAs aperture size while maintaining the same high gain performance. It is well known that in order to maximize η_a, RAs aperture geometry should directly correlate with the shape of the feed radiation pattern [17]. For example, circular shaped RA apertures are typically the best choice when a feed with rotationally symmetric radiation pattern is used. However, circular apertures are not a good choice for SmallSat applications since they suffer from low packing efficiency when compared to rectangular apertures (panel stacking). For a circular feed pattern, a hexagonal aperture could provide high η_a while also achieving high packing efficiency.

Advances in origami engineering have mathematically defined the theory and mechanics of origami folding patterns. This has led to the development of deployable structures with extremely high packing efficiency that use conforming hinges and simple deployment mechanisms [18], [19], and [20]. These developments have inspired RF engineers to design novel antennas with unique physical and electromagnetic features [21], [22], and [23]. Recently, origami RA designs have been proposed to achieve packable designs [24],

EM reconfigurability [25]–[27], and deployability [28], [29] for SmallSat applications. In this paper, we use origami to leverage the characteristics of FPRs by creating a deployable hexagonal RA aperture that achieves both high η_a and high packing efficiency.

III. THEORETICAL AND EFFICIENCY ANALYSIS

From classical antenna theory [30], it is known that the maximal theoretical directivity (D_0) is proportional to the antenna electrical size. In the case of a uniformly excited (amplitude and phase) aperture, the relation between directivity (D_0) and physical antenna surface area (A) is given by (1) where, λ is the wavelength calculated at the operation frequency.

$$D_0 = 4\pi \frac{A}{\lambda^2} \tag{1}$$

However, a physically large aperture by itself does not guarantee an RA with high gain. The maximum gain (G_0) of a RA system is limited by its aperture efficiency (η_a), as seen in (2).

$$G_0 = D_0 \eta_a \tag{2}$$

It can be seen that for a given antenna size A, an increase of η_a leads to a gain (G_0) increase. Furthermore, higher G_0 extends transmission distances and improves SNR. Moreover, when η_a is increased, a desired value of G_0 can be achieved using a smaller aperture area (A), which is very beneficial for space missions with limited space, such as, SmallSats. Also, smaller RA apertures can lead to the development of deployable RAs with high packing efficiency. Therefore, to develop deployable RAs with high packing efficiency, it is essential to investigate methods to improve η_a. In this section, we discuss the effect of aperture geometry on η_a and compare the efficiencies of the proposed Hexagonal Twist geometry to that of an ideal circular aperture.

A. APERTURE EFFICIENCY

RAs are spatially fed antennas, therefore, the dominating factors of η_a are the spillover efficiency (η_s) and illumination efficiency (η_i) efficiency [17]. Other factors that affect η_a depend on the unit cell-design, feed antenna matching, and polarization; these factors will be assumed ideal for the analysis in this section. With these assumptions, the equation for η_a can be written as (3).

$$\eta_a = \eta_s \eta_i \tag{3}$$

A study of the effects of the aperture's geometry on η_a was conducted in [8]. The study compared the maximum theoretical η_a of four different apertures (rectangular, square, circular, and hexagonal) considering a point source feed with rotationally symmetric radiation pattern. The results in [8] illustrated that the hexagonal topology provides similar η_a to the one of a circumscribed circular aperture, which is larger than the circumscribed square and rectangular apertures. However, due to its round edges, when a circular aperture is stowed, it leaves unused space inside the SmallSat bus, thereby reducing its packing efficiency. If a stowed aperture topology can utilize this idle space, it can increase its packing efficiency thereby increasing its physical deployed area, A, and directivity, D_0. To accomplish this, we designed here a deployable hexagonal aperture based on the modified hexagonal twist (MHT) origami folding pattern.

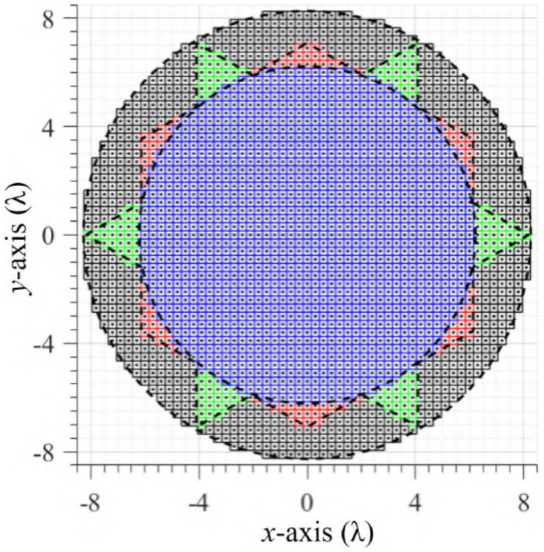

FIGURE 2. Four different RA aperture geometries in order of decreasing area: circular circumscribed (black), modified hexagonal twist (green), regular hexagonal (red), and circular inscribed (blue).

TABLE 1. Results of η_a study with array theory validation.

Aperture Geometry	A (λ^2)	η_s (%)	η_i (%)	η_a (%)	D_0 (dBi)	SLL (dB)
CC	215	88.6	86.3	76.5	33.8	-29.4
MHT	174	88.3	85.7	75.7	32.8	-27.0
RH	131	88.5	86.0	76.1	31.6	-27.4
IC	122	88.6	86.4	76.5	31.3	-27.8

Since the MHT aperture is more complex than a simple hexagonal aperture, we conducted an analytical study to compare its η_a to the efficiencies of the regular hexagonal (RH), a circular circumscribed (CC) and a circular inscribed (IC) apertures, as seen in Fig. 2. The analytical configuration considers a point source feed positioned at the broadside, whose power pattern is defined by $\cos^{2q}(\theta_f)$, as described in [17], with q-factor = 5.25. Then, the maximum theoretical η_a for each aperture in this configuration was found numerically by sweeping the height of the feed, H_f. The radiation pattern of each aperture was calculated analytically using array theory, [17], and the elevation plane cuts at $\phi = 0°$ are plotted in Fig. 3. The results of our analytical study are summarized in Table 1. It can be seen that the MHT and RH apertures achieve efficiencies, η_a, of 75.7% and 76.1%, respectively, which are comparable to the 76.5% efficiency of both circular apertures. Also, the MHT aperture exhibited

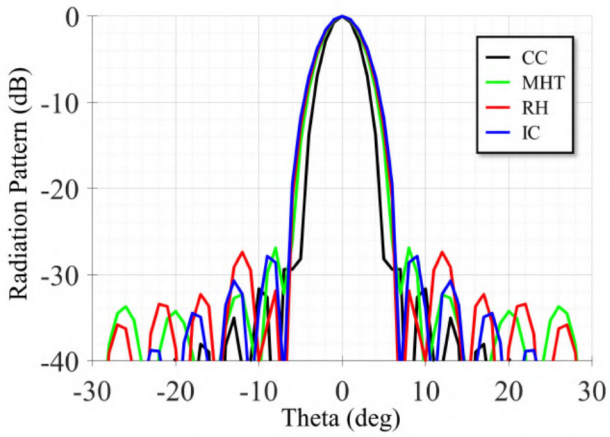

FIGURE 3. Normalized radiation patterns of four different RA aperture geometries analytically calculated (using array theory).

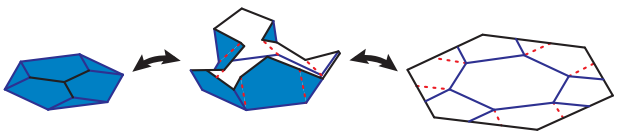

FIGURE 4. The folding motion of the hexagonal twist pattern from completely folded to partially unfolded to flat folded. The blue denotes the outside of each panel. The white denotes the inside of each panel. Mountain folds are denoted by solid, blue lines. Valley folds are denoted by dashed, red lines.

slightly lower η_a (only 0.4% less) than the RH one. This occurred because MHT has added points that extend past the points of the RH perimeter, which cause higher spillover and less uniformity in the amplitude distribution. However, the added points of the MHT increase its reflecting surface by 33%, thereby providing a 1.2 dB higher directivity than RH. Notably, MHT achieves this directivity improvement while maintaining the same stowed volume with RH. To summarize, MHT achieves high η_a (comparable to the ideal case of a circular aperture) while providing a high packing efficiency, such as, the one of rectangular apertures.

IV. ORIGAMI DESIGN

Origami has inspired engineers and designers to develop deployable systems that can provide structures with large deployed areas and compact stowed volumes [31]–[35]. Origami fold pattern motion is initially characterized using zero-thickness kinematic models because paper models have essentially zero-thickness. These kinematic models allow designers to determine not only the motion but how many inputs are required to actuate the patterns, or the degrees of freedom of the mechanism. Many origami fold patterns are one degree of freedom, meaning only one input must be applied to fully actuate the entire mechanism. This highly simplifies the actuation of a pattern over mechanisms with more degrees of freedom.

A. THICKNESS ACCOMMODATION TECHNIQUES

Zero-thickness models of origami provide valuable theoretical insight, but they alone do not provide the answers

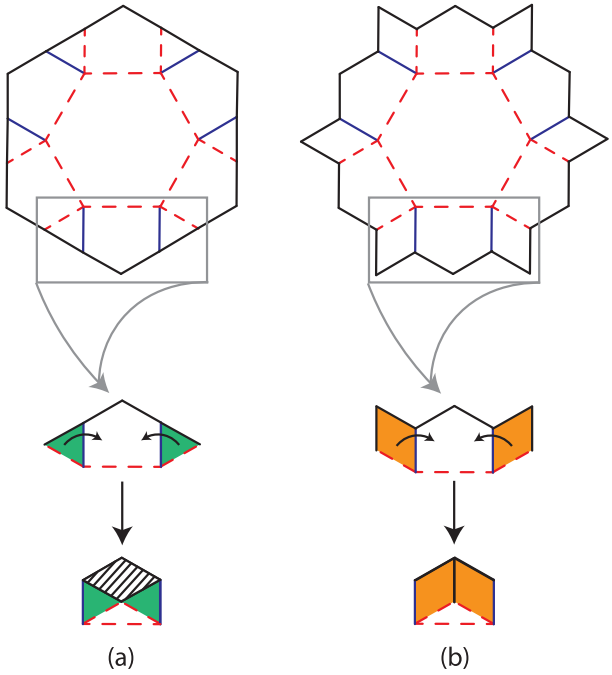

FIGURE 5. (a) The hexagonal twist pattern. The area of the pentagonal panel that the triangle panel (green) occupies when folded. The dashed area shows the portion of the panel area that could be covered without interfering with other panels during folding. (b) The modified hexagonal twist pattern. This pattern takes advantage of unused area in the original pattern. The area of the pentagonal panel that the rhombus (orange) occupies when folded. The rhombus occupies the maximum amount of area when folded without interfering with other folded panels.

for ways to fold materials with thickness. To alleviate this problem, multiple thickness accommodation techniques have been developed [36]. One of the earliest techniques to accommodate for thickness is the hinge-shift technique [37]. In this technique, the locations of the joints are moved from the zero-thickness plane, to the top and bottom planes of the thick mechanism. However, Tachi [38] discusses a drawback of this technique as only being applicable to a symmetric degree-4 vertex. This limitation can be worked around with the use of compliance in the system and thin panels.

The offset panel technique [39] provides a different method to accommodate for thickness while still keeping the joints at the same positions of the zero-thickness model. In this method, the panels are moved away from the initial zero-thickness plane specified distances to allow for nesting of the panels with each other. Although the panels are on different planes, for a flat-foldable pattern, these planes are all parallel.

B. ORIGAMI PATTERN INSPIRATION

The origami pattern that is basis of this work is the hexagonal twist as used in [40]. This pattern incorporates a central hexagonal panel which also is the footprint of the folded shape, as shown in Fig. 4. When opened, the central hexagonal panel is surrounded by alternating pentagonal panels on each edge and equilateral triangular panels on each point. This creates a larger hexagon, with the points rotated 60 degrees from their initial location in the folded pattern. This motion is illustrated in Fig. 4.

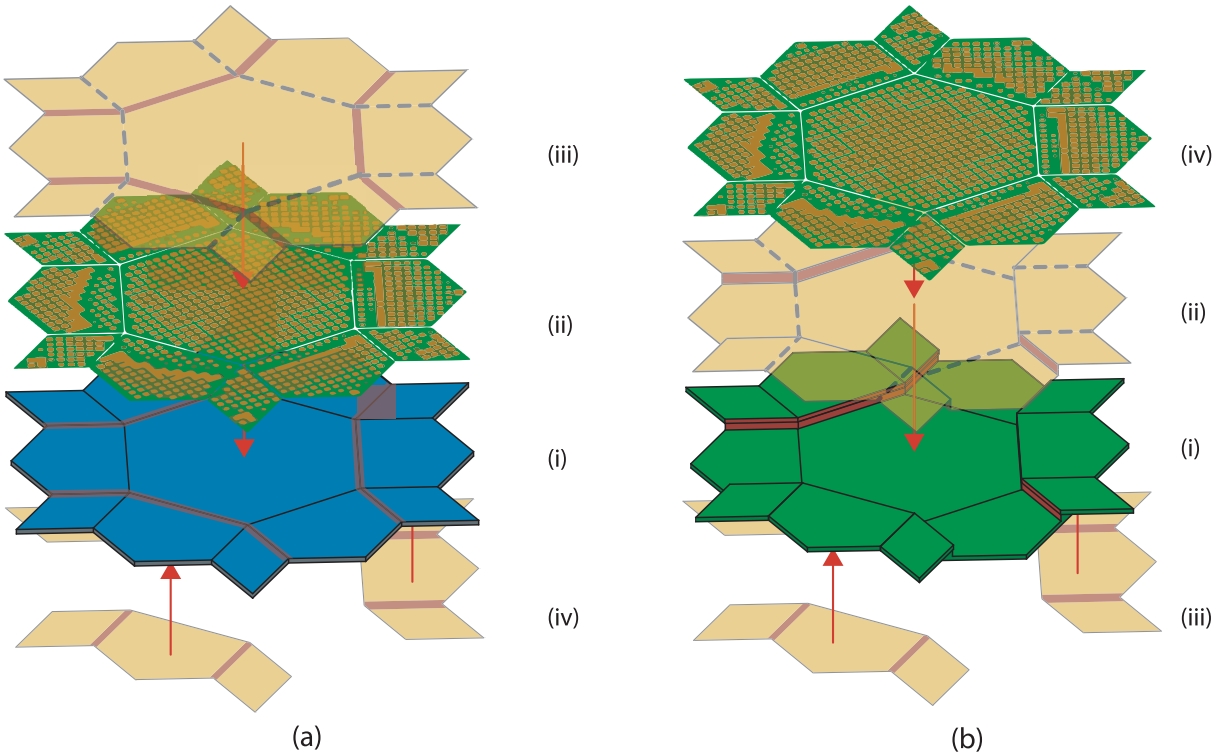

FIGURE 6. (a) The assembly procedure for the hexagonal RA made using the hinge shift technique. The EM panels (ii) are attached to the hexagonal twist mechanism (i). Membranes (iii) and (iv) are used to connect certain parts of the top and bottom of the pattern. The large dashed lines show where the membrane should be cut. (b) The assembly procedure for the hexagonal RA made using the offset panel technique. The hexagonal twist mechanism (i) is attached using membranes on the top (ii) and bottom (iii). The EM panels (iv) can then be attached. This method (b) allows the panels to be removed and replaced without disassembling the full mechanism. The red highlighted portions of the thickness accommodation techniques and the membranes show where the hinges in the designs are located.

C. MODIFIED HEXAGONAL TWIST

Because a larger aperture size is better in high gain antenna applications, the pattern was modified to increase the deployed area without increasing the stowed volume. As shown in Fig. 5, the triangular panels only cover a portion of the pentagonal panels when folded. Fig. 5(a) shows the additional area that could be covered by these panels, without interfering with the pattern in the open state. If this area is divided between each triangular panel equally, the panels end up as rhombi. This creates a deployed shape of a hexagon with six extending points, increasing the deployed surface area of the pattern by $14.49\lambda^2$, or 33%.

V. MECHANICAL DESIGN

The modified hexagonal twist pattern is applied here to reflectarray antennas. The hinge shift and offset panel thickness accommodation techniques are applied to the pattern to create two different approaches to the antenna. The benefits and limitations of each accommodated hexagonal reflectarray (RA) are discussed below.

A. HINGE SHIFT THICKNESS ACCOMMODATED HEXAGONAL TWIST RA

The hinges shift thickness accommodation technique is applied to the hexagonal twist pattern. Although this technique normally cannot be applied to patterns with non-symmetric vertices and nesting of more than one set of panels, certain approaches can be used to incorporate it into this pattern.

First, to use this technique with this mechanism, the thickness of the mechanism must be much smaller than

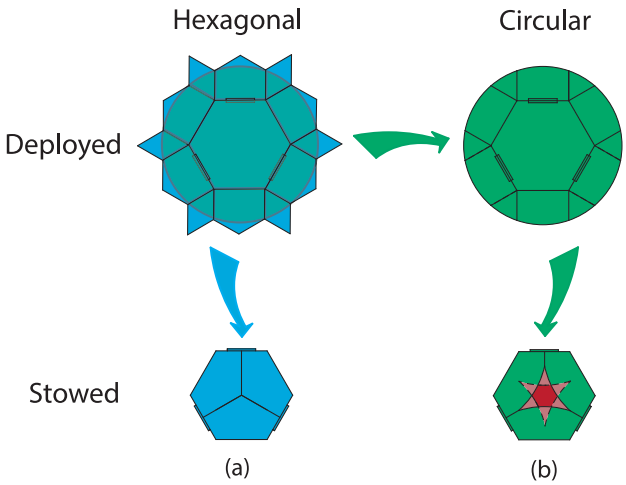

FIGURE 7. (a) The hexagonal twist array in the deployed and stowed states. The green circular highlight shows the largest circular aperture that can be cut and folded using the hexagonal twist pattern. (b) The deployed and stowed states of the circular aperture using the hexagonal twist fold pattern. The stowed state is less efficiently packed compared to the hexagonal twist array. The red inner portions show the volumes that are not filled in the circular array compared to the hexagonal array. The lighter red signifies one thickness of material missing and the dark red signifies two thicknesses of material that are missing.

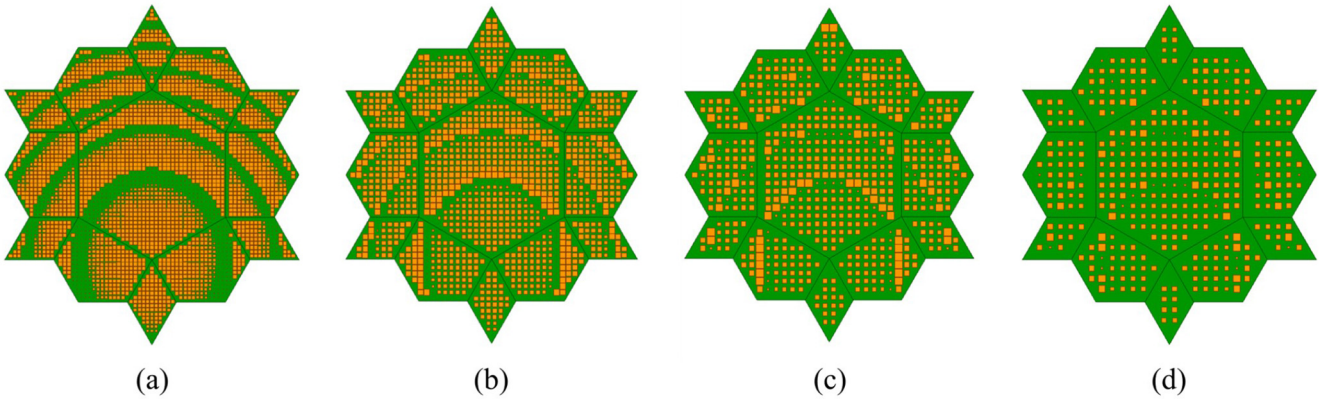

FIGURE 8. Hexagonal twist aperture discretized with different UC dimensions: (a) $L = 0.2\lambda$, (b) $L = 0.3\lambda$, (c) $L = 0.4\lambda$, and (d) $L = 0.5\lambda$.

TABLE 2. Packing efficiency of hexagonal and circular apertures.

	Hexagonal	Circular
Packing Efficiency	0.75	0.61
Deployed Area to Stowed Volume	0.74	0.53

the planar dimensions of the panels (lengths and widths). Second, to account for the set of pentagonal panels that fold on the outside of the pattern (perpendicularly to the initial plane), the hinges of these panels need to be removed to increase the mobility of the origami mechanism [41].

This method provides for an antenna that can operate at a single state (i.e., its unfolded state). The hinges need to be applied to the top layer (above the microstrip RA panels) and the bottom surface. Notably, this technique provides for an antenna where all microstrip RA panels are on the same plane in the deployed position.

B. OFFSET PANEL THICKNESS ACCOMMODATED HEXAGONAL TWIST RA

The offset panel thickness accommodation technique is also applied to the hexagonal twist pattern. This technique preserves the kinematics of the initial zero-thickness pattern. Additionally, this technique can accommodate for any thickness of the microstrip RA panels used in the RA design. This enables the hexagonal mechanism to be assembled prior to mounting the microstrip RA panels onto the mechanism. This technique can be used for designs that require a more modular design approach because the microstrip RA panels can be effectively placed and removed without taking apart the entire RA. These RA panels could be easily replaced with a different design if desired.

This method, however, creates an RA with panels on different planes. This could lead to more challenging EM analysis and design. The assembly procedure of the hexagonal array based on this thickness accommodation method is shown in Fig. 6(b).

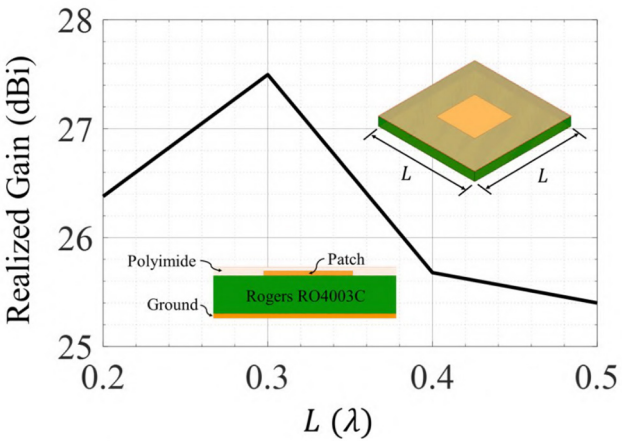

FIGURE 9. Effect of unit-cell size on gain of a hexagonal twist RA aperture.

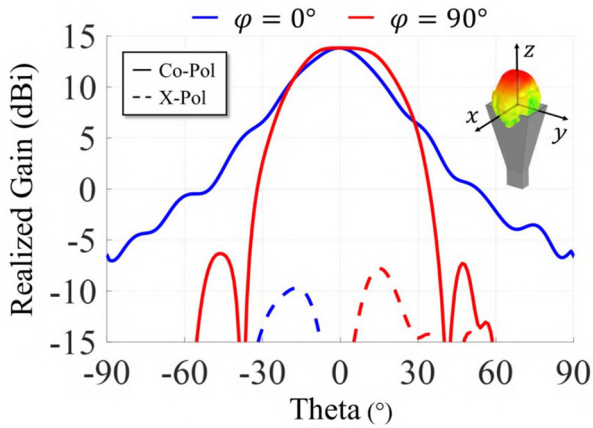

FIGURE 10. Two principal planes of the MVG SH2000 horn antenna feed radiation pattern.

C. HINGE DESIGN

Membrane hinges were used in these design cases because of their ability to provide flexibility about the axis of desired motion while inhibiting motion in undesired directions. The panel edges in both techniques can provide mechanical hard

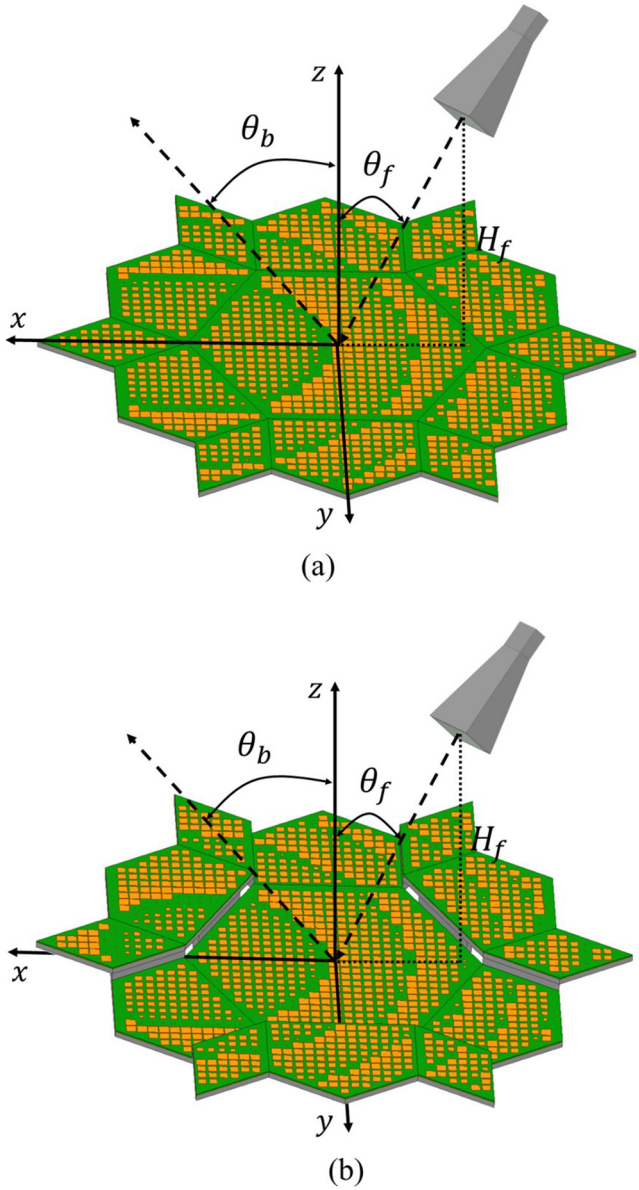

FIGURE 11. RA models for (a) flat RA aperture and (b) offset RA aperture.

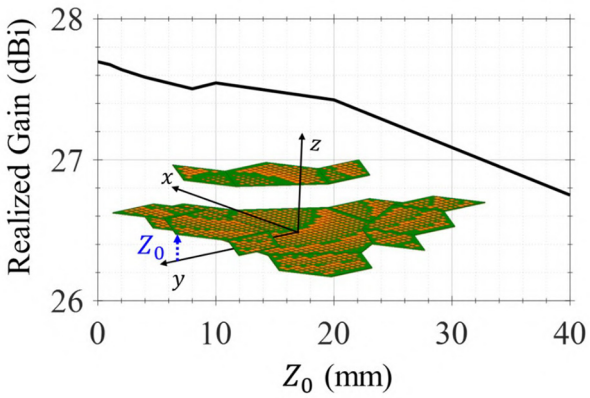

FIGURE 12. Effect of panel offset on realized gain.

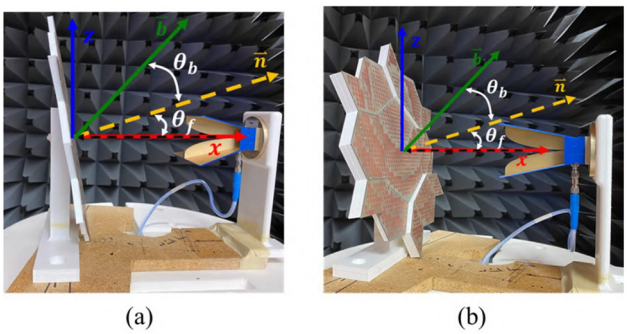

FIGURE 13. Measurement setup for (a) flat RA aperture, and (b) offset RA aperture.

stops that orient the panels to their final positions. The corners of the panels could be rounded to reduce chances of damage to the membrane or other systems. The hinge-shift and offset panel techniques are demonstrated here because of the advantages stated in the sections above, but other thickness accommodation techniques are also feasible [37].

D. PACKING EFFICIENCY

As discussed above, a circular aperture is more efficient than apertures of other shapes. The hexagonal twist pattern presented in this paper could be turned into a circular aperture to improve the efficiency of the reflectarray. Fig. 7 shows the hexagonal twist pattern and the largest circular pattern that could be cut from it, while still maintaining a shape that will completely fold flat. Fig. 7 also shows both apertures folded. In Fig. 7(b), the red portions of the stowed pattern show volumes contained in the hexagonal aperture that are missing in the circular aperture. This leads to a reflectarray that is using the volume less efficiently. Looking at the packing efficiency as the volume of the array divided by the volume of the smallest box that the stowed array could fit in, these apertures discussed here have packing efficiencies as shown in Table 2. Additionally, the deployed area compared to the volume of the smallest box the arrays could fit in when stowed was determined. Table 2 shows these values for both apertures. In both cases the hexagonal aperture is superior to the circular aperture.

E. DEPLOYMENT

Because this pattern is one degree-of-freedom (DOF), theoretically only one actuator would be needed to fully actuate the pattern. These actuation methods could range from using strain energy stored within at least one hinge to external actuation by a motor or extension booms, or other methods as discussed in [42]. While [43] specifically discusses actuation in regards to Miura-ori, many of these actuation methods could be tailored to work with the proposed hexagonal reflectarrays.

VI. EM DESIGN, FABRICATION, AND PERFORMANCE

Once the modified hexagonal twist origami structures were developed and validated, the next step was to implement

TABLE 3. Results of near-field measurement at 16 GHz.

	Flat		Offset	
Parameters	Sim	Meas	Sim	Meas
Gain (dBi)	27.5	26.4	27.5	26.8
η_a (%)	77.2	59.9	77.2	65.7
SLL (dB)	-22.4	-19.1	-22.5	-18.5
XPD (dB)	-32.6	-18.9	-34.4	-20.4
HPBW (°)	6	6	6	6

them as RA aperture system. To accomplish this, printed microstrip RA panels were designed to fit on the surfaces of the deployed origami structure. The panels were then modeled and simulated using ANSYS HFSS full-wave simulation software. Once the novel RA systems were validated using our simulation results, prototypes were fabricated and measured. In this section, the designs, simulation, prototype fabrication, and measurement process are discussed. Additionally, the results, simulated and measured, are presented and discussed.

A. UNIT-CELL DESIGN AND CHARACTERIZATION

The proposed aperture designs consist of 13 individual PCB panels and 18 fold lines. Therefore, the unit-cell size must be optimized to minimize the phase error introduced by the absence of unit-cells near the structure hinges. Hence, several MHT apertures were modeled and simulated using various unit-cell sizes (L) between 0.2λ to 0.5λ, as shown in Fig. 8. The maximum gain of the MHT RA for each case is presented in Fig. 9. It can be seen that the maximum gain is achieved when $L = 0.3\lambda$. Theoretically, a smaller L will result in higher phase resolution over the aperture leading to higher directivity. However, a smaller L reduces the inter element spacing, thereby increasing the effects of mutual coupling and leading to degradation of the antenna pattern [44].

In this work, both RA apertures (the RA based on the hinge shift technique, and the RA based on the offset panel technique) are synthesized using $L = 0.3\lambda$ square lattice with an operating frequency of 16 GHz. The substrate chosen is 0.81mm thick Rogers RO4003C laminate ($\epsilon_r = 3.55$ and $tan\delta = 0.0027$), and the phasing elements are square patches with variable size. Furthermore, the effect of a 5 mil polyimide layer, Kapton ($\epsilon_r = 3.4$ and $tan\delta = 0.002$), is also modeled to account for the membrane hinge used on the flat structure. With these design parameters, the unit-cell performance was characterized using the procedure described in [24]. It was found that when the patch size is swept from 0.15mm to 0.35mm, the unit-cell exhibits a maximum phase range of 322.5° and 325.5° and a maximum loss of 0.34 dB and 0.69 dB for the case of with and without the membrane layer respectively. Although full 360° phase range is not achieved, this unit-cell is simple and adequate for the purposes of this study.

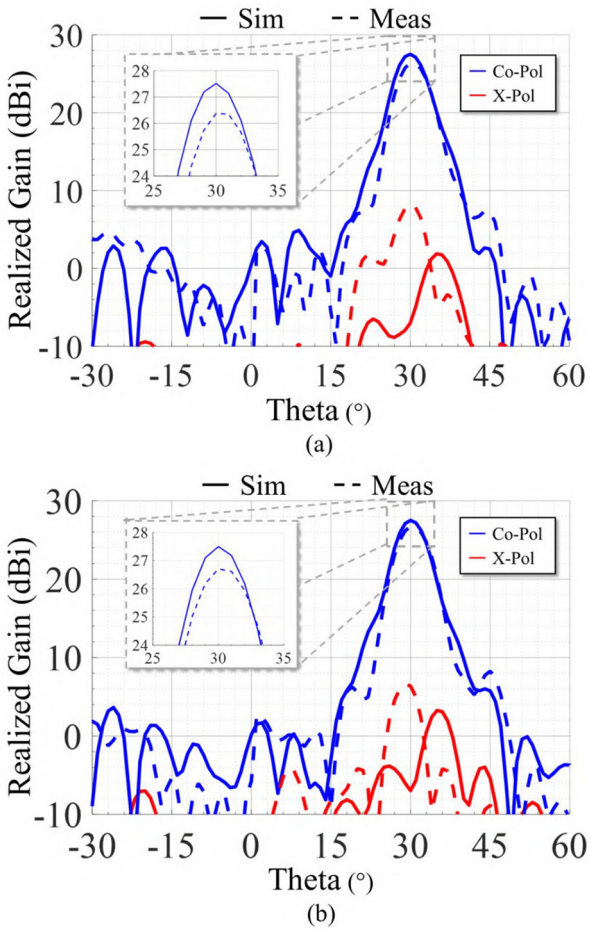

FIGURE 14. Comparison between simulation and measurements for a principle elevation plane ($\phi = 0°$) (a) flat RA aperture (b) offset RA aperture.

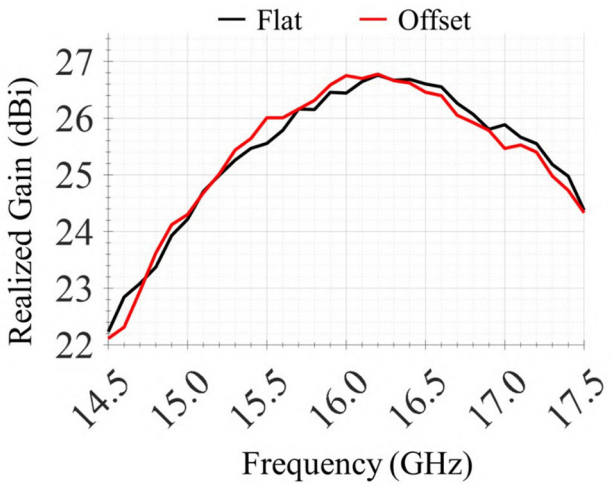

FIGURE 15. Realized gain in the desired direction ($\theta_b = 30°$, $\phi_b = 0°$) for both flat and offset structures.

B. FEED ANTENNA MODEL AND RA SYNTHESIS

In this work, an MVG SH2000 dual-ridge horn is used as the feed antenna for our RAs. To model the feed in our

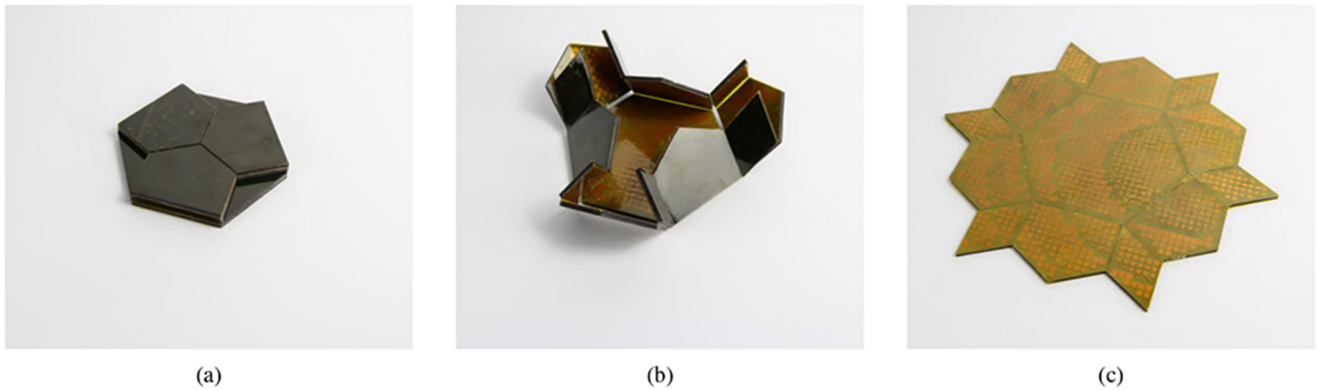

FIGURE 16. Hexagonal twist RA prototype using the hinge-shift thickness accommodation technique. The black structure is 3D printed PLA. The attached panels are the EM RA panels. A polyimide membrane is attached to the front and back of the mechanism. (a) Stowed, flat-folded state. (b) Partially folded/deployed state. (c) Fully deployed, flat state.

simulations, the feed was measured in an MVG StarLab near-field measurement system, and the measurement results were imported into ANSYS HFSS. The feed exhibits a maximum gain of 13.7 dB corresponding to a q-factor of 5.25, as shown in Fig. 10. Furthermore, the feed exhibits a maximum SLL of -20.3 dB, and a cross-polarization discrimination (XPD) of -38.4 dB. Then, the optimal feed position, was calculated considering the feed antenna pattern numerically. The feed is placed at a height $H_f = 9.4\lambda$ from the center of the RA, and an offset angle (θ_f) of 10° is implemented to minimize feed blockage, as shown in Fig. 11. This RA configuration has a focal ratio f/D of 0.58, and efficiencies η_s, η_i, and η_a of 88.3%, 88.9%, and 78.5%, respectively.

The RA panels were designed to direct the main beam direction ($\theta_b = 30°$, $\phi_b = 0°$) by calculating the unit-cell phase distribution using the ray-tracing method [17]. Then, complete RA models for each thickness accommodation method were developed: one with a flat aperture, and one with an offset aperture corresponding to the hinge shift, and the offset panel techniques described above, respectively, as shown in Fig. 11.

C. EFFECT OF OFFSET THICKNESS

To study the effect of placing unit-cells on separate planes, as it is done in the offset panel thickness accommodation technique, several apertures were modeled with varying values of panel offset, Z_0, as seen in Fig. 12. For each case of Z_0, a new RA was synthesized using the same design parameters and procedures described in Sections VI-A to VI-B. The maximum gain of each aperture as a function of Z_0 is shown in Fig. 12. In every case, the RA exhibited SLL < -20 dB, cross polarization discrimination (XPD) > 20 dB, and the main beam was pointed to the desired direction ($\theta_b = 30°$, $\phi_b = 0°$). It can be seen that increasing the offset of the panels up to a value of 20mm ($\sim 1\lambda$) does not significantly affect the performance of this structure (the losses are $<$0.5 dB). The performance does begin to decay more after at a distance $> 1\lambda$, partially due to the shadowing effect of the offset planes. For our RA design with the offset aperture, $Z_0 = 8$mm was chosen to accommodate the thickness of the substrate while maintaining a high packing efficiency.

D. PROTOTYPE AND FABRICATION

Prototypes were constructed for both the flat and offset RAs. In each case, the hexagonal twist mechanism was made from 3D printed polylactic acid (PLA). The microstrip RA panels were fabricated from Rogers RO4003C laminate using an LPKF ProtoLaser U4 laser milling machine. The microstrip RA panels were then affixed to the PLA mechanism using epoxy adhesive. The hinges of the flat structure were made using 5 mil Kapton membrane as described in Section V-A. Meanwhile, the hinges of the offset-panel prototype were made using spinnaker tape membrane as described in Section V-B. The two RA prototypes at their stowed, partially deployed, and fully deployed states are shown in Figs. 16 and 17.

E. REFLECTARRAY PERFORMANCE

The measurements were done in an MVG near-field measurement system. The measurement setup for both RA structures is shown in Fig. 13. The measured results are compared to the simulated ones in Fig. 14 and summarized in Table 3. Our proposed RAs achieved a total realized gain of 26.4 dBi and 26.8 dBi, corresponding to a calculated η_a of 59.9% and 65.7%, for the flat and offset structures, respectively. The additional losses and reduction in η_a when compared to the simulation is due to phase, quantization, and polarization errors caused by the materials, fabrication tolerances, and alignment of the apertures in the measurement setup. A frequency sweep was also performed to measure the realized gain in the designed direction ($\theta_b = 30°$, $\phi_b = 0°$) at intervals of 100 MHz in the range of 14.5 to 17.5 GHz, as seen in Fig. 15. The 1 dB bandwidth of the flat and offset apertures is 8.9% and 9.0%, respectively. In both cases, both the SLL and XPD are maintained at approximately -20 dB. The prototypes exhibited higher levels of XPD than in simulation due to alignment errors in the prototype fabrication and measurement setup.

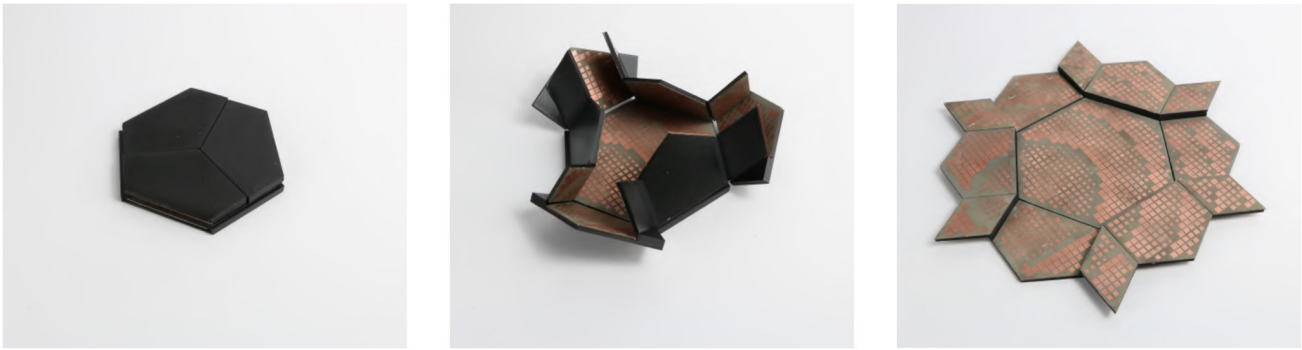

(a) (b) (c)

FIGURE 17. Hexagonal twist RA prototype using the offset panel thickness accommodation technique. (a) Stowed, flat-folded state. (b) Partially folded/deployed state. (c) Fully deployed, flat state.

TABLE 4. Comparison between flat and offset hexagonal twist apertures.

	Flat		Offset	
	Pros	**Cons**	**Pros**	**Cons**
Electromagnetic	• All unit-cells lie on a single plane → closer to infinite array assumption → lower phase errors • Single connected plane increases η_s	• Membrane hinge on the surface adds losses to the system • Edge tapering causes lower η_i	• Offset of the edge elements increases η_i	• Panel offset causes aperture shadowing and decreases η_s
Mechanical	• Planar manufacturing from single sheet of material • Lower mass	• Accommodation technique only works for thin arrays ($t << other\ dimensions$) • Less panel support in the open state → less stability	• Assembly allows for modular design (arrays could be replaced easily) • Increased panel support in the open state → higher stability	• Higher mass • Complex parts

A summary of the pros and cons of each aperture is provided in Table 4. The flat aperture exhibits higher losses (0.4 dB) and lower XPD (1.5 dB) when compared to the offset aperture. The higher losses in the flat aperture can be attributed to the Kapton membrane hinge that lies on top of the phasing elements, but also to polarization errors caused by misalignment of the panels during the fabrication process, evidenced by the lower XPD. Additionally, the membrane layer caused the flat RA to experience a 300 MHz frequency shift, likely caused by air pockets observed in the application of the membrane layer. Therefore, in terms of electromagnetic performance, the offset aperture outperformed the flat aperture due to two factors: (1) panel offset does not significantly affect RA performance when the offset is small relative to the focal distance of the feed, and (2) the membrane hinge in the offset structure is placed behind the ground plane. However, there are mechanical advantages and disadvantages to each of the structures. For example, the flat aperture has a lower mass and can be manufactured from a single sheet of material with uniform thickness, but it is less stable in its deployed state than the offset aperture. Meanwhile, the offset aperture is more stable in its deployed state and supports modular designs by allowing microstrip panels to be swapped out, but it has larger mass and requires custom parts.

VII. CONCLUSION

A deployable RA system based on an origami folding pattern was introduced here to improve the aperture and packing efficiencies of traditional deployable RAs. The design process of rigid-foldable structures with thickness accommodation was discussed and the hexagonal twist folding pattern was modified to develop two novel deployable RA apertures. The

surfaces of the panels in these structures were affixed to the phasing elements to create a deployable RA aperture with high packing efficiency and aperture efficiency. The effects of unit-cell size were studied to achieve the optimal gain for this type of structure. The effects of panel offset were studied and it was found that it does not significantly affect the performance of the RA system. Our RA's performance showed that at the deployed state, the RA apertures operate at 16 GHz and achieved a gain of 26.4 dBi and 26.8dBi, for the flat and offset structures respectively. The apertures were designed for 16 GHz, but they are scalable to many different frequency bands. Both apertures exhibited low SLL and good XPD of approximately −20 dB for metrics. It was found that the offset aperture provides higher gain and more structural stability than the flat aperture. However, the flat aperture has a lower mass and can be fabricated from a single sheet of material. Both apertures have demonstrated high volume packing efficiency, 75%, and high aperture efficiency, at least 60%, with simple deployment mechanism using a single actuator thereby making them good candidates for SmallSat and tactical applications.

ACKNOWLEDGMENT

The authors would like to thank Hunter Pruett for assistance in assembling the prototypes and Nathan Brown for assistance with photographing the prototypes.

REFERENCES

[1] G. Curzi, D. Modenini, and P. Tortora, "Large constellations of small satellites: A survey of near future challenges and missions," *Aerospace*, vol. 7, no. 9, p. 133, 2020.

[2] I. Del Portillo, B. G. Cameron, and E. F. Crawley, "A technical comparison of three low earth orbit satellite constellation systems to provide global broadband," *Acta Astronautica*, vol. 159, pp. 123–135, Jun. 2019.

[3] N. Chahat, R. E. Hodges, J. Sauder, M. Thomson, and Y. Rahmat-Samii, "The deep-space network telecommunication cubesat antenna: Using the deployable ka-bandmesh reflector antenna," *IEEE Antennas Propag. Mag.*, vol. 59, no. 2, pp. 31–38, Apr. 2017.

[4] A. Jacomb-Hood and E. Lier, "Multibeam active phased arrays for communications satellites," *IEEE Microw. Mag.*, vol. 1, no. 4, pp. 40–47, Dec. 2000.

[5] R. E. Hodges, D. J. Hoppe, M. J. Radway, and N. E. Chahat, "Novel deployable reflectarray antennas for cubesat communications," in *Proc. IEEE MTT-S Int. Microw. Symp.*, 2015, pp. 1–4.

[6] R. E. Hodges, B. Shah, D. Muthulingham, and T. Freeman, *ISARA—Integrated Solar Array and Reflectarray Mission Overview*, NASA/JPL (Jet Propulsion Lab.), Pasadena, CA, USA, 2013.

[7] R. E. Hodges, N. Chahat, D. J. Hoppe, and J. D. Vacchione, "A deployable high-gain antenna bound for mars: Developing a new folded-panel reflectarray for the first cubesat mission to mars," *IEEE Antennas Propag. Mag.*, vol. 59, no. 2, pp. 39–49, Apr. 2017.

[8] A. J. Rubio, A.-S. Kaddour, S. V. Georgakopoulos, C. Ynchausti, S. Magleby, and L. L. Howell, "A deployable hexagonal reflectarray antenna for space applications," in *Proc. United States Nat. Committee URSI Nat. Radio Sci. Meeting (USNC-URSINRSM)*, 2021, pp. 136–137.

[9] Y. Rahmat-Samii, V. Manohar, and J. M. Kovitz, "For satellites, think small, dream big: A review of recent antenna developments for CubeSats.," *IEEE Antennas Propag. Mag.*, vol. 59, no. 2, pp. 22–30, Apr. 2017, doi: 10.1109/MAP.2017.2655582.

[10] N. Chahat, R. E. Hodges, J. Sauder, M. Thomson, E. Peral, and Y. Rahmat-Samii, "CubeSat deployable Ka-band mesh reflector antenna development for earth science missions," *IEEE Trans. Antennas Propag.*, vol. 64, no. 6, pp. 2083–2093, Jun. 2016, doi: 10.1109/TAP.2016.2546306.

[11] M. Hwang, G. Kim, S. Kim, and N. S. Jeong, "Origami-inspired radiation pattern and shape reconfigurable dipole array antenna at C-band for CubeSat applications," in *IEEE Trans. Antennas Propag.*, vol. 69, no. 5, pp. 2697–2705, May 2021, doi: 10.1109/TAP.2020.3030908.

[12] N. Chahat *et al.*, "Advanced CubeSat antennas for deep space and earth science missions: A review," *IEEE Antennas Propag. Mag.*, vol. 61, no. 5, pp. 37–46, Oct. 2019.

[13] M. Cooley *et al.*, "RF design and development of a deployable membrane reflectarray antenna for space," in *Proc. IEEE Int. Symp. Phased Array Syst. Technol. (PAST)*, 2019, pp. 1–4.

[14] J. Huang and A. Feria, "Inflatable microstrip reflectarray antennas at X and Ka-band frequencies," in *IEEE Antennas Propag. Soc. Int. Symp. Dig. Held Conjunction USNC/URSINational Radio Sci. Meeting*, vol. 3, 1999, pp. 1670–1673.

[15] H. Fang, J. Huang, U. Quijano, K. Knarr, J. Perez, and L.-M. Hsia, "Design and technologies development for an eight-meter inflatable reflectarray antenna," in *Proc. 47th AIAA/ASME/ASCE/AHS/ASC Struct. Struct. Dyn. Mater. Conf. 14th AIAA/ASME/AHS Adapt. Struct. Conf.*, 2006, p. 2230.

[16] R. E. Hodges, M. J. Radway, A. Toorian, D. J. Hoppe, B. Shah, and A. E. Kalman, "ISARA—Integrated solar array and reflectarray cubesat deployable Ka-band antenna," in *Proc. IEEE Int. Symp. Antennas Propag. USNC/URSI Nat. Radio Sci. Meeting*, 2015, pp. 2141–2142.

[17] P. Nayeri, F. Yang, and A. Z. Elsherbeni, *Reflectarray Antennas: Theory, Designs, and Applications*. New York, NY, USA: Wiley, 2018.

[18] R. J. Lang, *Twists, Tilings, and Tessellations: Mathematical Methods for Geometric Origami*. Boca Raton, FL, USA: CRC Press, 2017.

[19] R. J. Lang, T. Nelson, S. Magleby, and L. Howell, "Thick rigidly foldable origami mechanisms based on synchronized offset rolling contact elements," *J. Mech. Robot.*, vol. 9, no. 2, 2017, Art. no. 021013.

[20] Z. Zhai, Y. Wang, and H. Jiang, "Origami-inspired, on-demand deployable and collapsible mechanical meta-materials with tunable stiffness," *Proc. Nat. Acad. Sci.*, vol. 115, no. 9, pp. 2032–2037, 2018.

[21] S. V. Georgakopoulos, "Reconfigurable origami antennas," in *Proc. Int. Appl. Comput. Electromagn. Soc. Symp. (ACES)*, 2019,pp. 1–2.

[22] S. I. H. Shah and S. Lim, "Review on recent origami inspired antennas from microwave to terahertz regime," *Mater. Design*, vol. 198, Jan. 2021, Art. no. 109345.

[23] S. V. Georgakopoulos *et al.*, "Origami antennas," *IEEE Open J. Antennas Propag.*, vol. 2, pp. 1020–1043, 2021, doi: 10.1109/OJAP.2021.3121102.

[24] A. J. Rubio *et al.*, "An origami-inspired foldable reflectarray on a straight-major square-twist pattern," in *Proc. IEEE 21st Annu. Wireless Microw. Technol. Conf. (WAMICON)*, 2021, pp. 1–4.

[25] A.-S. Kaddour, C. A. Velez, and S. V. Georgakopoulos, "A deployable and reconfigurable origami reflectarray based on the Miura-Ori pattern," in *Proc. IEEE Int. Symp. Antennas Propag. North Amer. Radio Sci. Meeting*, 2020,pp. 91–92.

[26] A.-S. Kaddour, C. L. Zekios, and S. Georgakopoulos, "Reconfigurable arrays with multiple unit cells," U.S. Patent 10 931 022, Feb. 2021.

[27] C. A. Velez *et al.*, "Reconfigurable and deployable Miura-Ori RA analysis for satellite applications," in *Proc. IEEE 21st Annu. Wireless Microw. Technol. Conf. (WAMICON)*, 2021, pp. 1–3.

[28] A.-S. Kaddour *et al.*, "A foldable and reconfigurable monolithic reflectarray for space applications," *IEEE Access*, vol. 8, pp. 219355–219366, 2020.

[29] N. Miguélez-Gómez *et al.*, "Thickness-accommodation in X-band origami-based reflectarray antenna for small satellites applications," in *Proc. IEEE Int. Conf. Wireless Space Extreme Environ. (WiSEE)*, 2020, pp. 54–59.

[30] C. A. Balanis, *Antenna Theory: Analysis and Design*. Hoboken, NJ, USA: Wiley, 2015.

[31] S. R. Woodruff and E. T. Filipov, "Structural analysis of curved folded deployables," in *Earth and Space 2018: Engineering for Extreme Environments*. Reston, VA, USA: Amer. Soc. Civil Eng., 2018, pp. 793–803.

[32] S. Jagarlapudi, S. Siddapureddy, and D. V. Patil, "On the use of origami for solar energy harvesting," in *Advances in Solar Energy Research*. Singapore: Springer, 2019, pp. 317–330.

[33] M. E. H. Bhuiyan, D. Semer, and B. P. Trease, "Parametric studies of geometric design factors on static and dynamic loading of an origami flasher," in *Proc. SmartMater. Adapt. Struct. Intell. Syst.*, vol. 58257, 2017, Art. no. V001T08A016.

[34] S.-M. Baek, S. Yim, S.-H. Chae, D.-Y. Lee, and K.-J. Cho, "Ladybird beetle-inspired compliant origami," *Sci. Robot.*, vol. 5, no. 41, 2020, Art. no. eaaz6262.
[35] R. Wu, P. C. Roberts, L. Xu, C. Soutis, and C. Diver, "Deployable self-regulating centrifugally-stiffened decelerator (descent): Design scalability and low altitude drop test," *Aerosp. Sci. Technol.*, vol. 114, Jul. 2021, Art. no. 106710.
[36] E. A. P. Hernandez, D. J. Hartl, and D. C. Lagoudas, "Introduction to active origami structures," in *Active Origami*. Cham, Switzerland: Springer, 2019, pp. 1–53.
[37] R. J. Lang, K. A. Tolman, E. B. Crampton, S. P. Magleby, and L. L. Howell, "A review of thickness-accommodation techniques in origami-inspired engineering," *Appl. Mech. Rev.*, vol. 70, no. 1, 2018, Art. no. 010805.
[38] C. S. Hoberman, "Reversibly expandable three-dimensional structure," U.S. Patent 4 780 344, Oct. 25 1988.
[39] T. Tachi, "Rigid-foldable thick origami," *Origami*, vol. 5, pp. 253–264, Jun. 2011.
[40] B. J. Edmondson, R. J. Lang, S. P. Magleby, and L. L. Howell, "An offset panel technique for thick rigidily foldable origami," in *Proc. Int. Design Eng. Tech. Conf. Comput. Inf. Eng. Conf.*, vol. 46377, 2014, Art. no. V05BT08A054.
[41] K. A. Tolman, R. J. Lang, S. P. Magleby, and L. L. Howell, "Split-vertex technique for thickness-accommodationin origami-based mechanisms," in *Proc. Int. Design Eng. Tech. Conf. Comput. Inf. Eng. Conf.*, 2017, Art. no. V05BT08A054.
[42] A. Yellowhorse and L. L. Howell, "Creating rigid foldability to enable mobility of origami-inspired mechanisms," *J. Mech. Robot.*, vol. 8, no. 1, 2016, Art. no. 011011.
[43] D. Bolanos *et al.*, "Considering thickness-accommodation, nesting, grounding and deployment in design of Miura-Ori based space arrays," in *Proc. 5th ASME/IFToMM Int. Conf. Reconfig. Mech. Robots*, 2021.
[44] Y. Abdallah, C. Menudier, M. Thevenot, and T. Monediere, "Investigations of the effects of mutual coupling in reflectarray antennas," *IEEE Antennas Propag. Mag.*, vol. 55, no. 2, pp. 49–61, Apr. 2013.

ANTONIO J. RUBIO (Graduate Student Member, IEEE) graduated from Naval Nuclear Power Training Command Power School in 2011, and Naval Power Training Unit, Charleston, SC, USA, in 2012, before serving on the USS Providence (SSN-719). He received the B.S. degree in electrical engineering from Florida International University, Miami, FL, USA, in 2019, where he is currently pursuing the Ph.D. degree in electrical and computer engineering. He is currently serving as a Graduate Research Assistant with the Transforming Antennas Center, FIU. His research is focused on RF systems, communications, deployable and reconfigurable antennas, reflectarrays, and machine learning optimization.

ABDUL-SATTAR KADDOUR (Member, IEEE) received the B.S. degree in electronics from the Lebanese University, Faculty of Science, Lebanon, in 2011, the B.S. and M.S. degrees in electronics and embedded systems engineering from the Grenoble Institute of Technology, Grenoble, France, in 2012 and 2014, respectively, and the Ph.D. degree in optics and radiofrequency from the Grenoble Alpes University, Grenoble, France, in 2018. His Ph.D. has been realized at CEA-LETI, Grenoble, France, where he developed electrically small and frequency reconfigurable antennas for space applications. In 2018, he joined the Xlim Research Institute, Limoges, France. Since 2019, he has been a Research Fellow with the Transforming Antennas Center, Florida International University, Miami, FL, USA. He has four issued patents in the U.S. Patent Office. His main research interests include electrically small antennas, reconfigurable antennas, antenna arrays, reflectarrays, and wireless power transfer systems. He serves as a reviewer for the numerous IEEE journals in the field of microwave, antennas, and propagation.

COLLIN YNCHAUSTI received the B.S. degree in mechanical engineering from the University of Utah, Salt Lake City, UT, USA, in 2015. He is currently pursuing the Ph.D. degree in mechanical engineering with Brigham Young University, Provo, UT, USA. Prior to BYU, he was a Product Line Engineer with Bechtel Marine Propulsion Corporation. He is currently a Research Assistant with the Compliant Mechanism Research Group, Brigham Young University researching compliant mechanisms and deployable systems.

SPENCER MAGLEBY received the B.S. and M.S. degrees in civil engineering from BYU and the Ph.D. degree in mechanical engineering from the University of Wisconsin–Madison. He is a Professor of Mechanical Engineering with Brigham Young University, where he is currently the Honors Program Director. He spent six years in the military aircraft industry developing tools for advanced aircraft design and manufacture. At BYU, he has pursued research in areas of product design, technology development and engineering education and has been especially active in developing new technologies and applications related to compliant mechanisms and the use of origami to inspire innovative product design. He teaches design at the graduate and undergraduate level. He is an Avid Road Cyclist, an Amateur Architect, and a Design Junkie.

LARRY L. HOWELL received the B.S. degree from Brigham Young University (BYU) and the M.S. and Ph.D. degrees from Purdue University. He is a Professor and an Associate Academic Vice President with BYU. Prior to joining BYU, he was with Engineering Methods and an Engineer on the YF-22 (the prototype for the U.S. Air Force F-22 Raptor). His research focuses on compliant mechanisms, including origami-inspired mechanisms, space mechanisms, and medical devices. He is a recipient of the ASME Machine Design Award, the ASME Mechanisms and Robotics Award, the Theodore von Kármán Fellowship, the NSF Career Award, the Purdue Outstanding Mechanical Engineer (Alumni Award), and the BYU Karl G. Maeser Distinguished Lecturer Award (BYU's Highest Faculty Award). He is the Co-Editor of the *Handbook of Compliant Mechanisms* and has authored *Compliant Mechanisms* which are published in English and Chinese. His lab's work has also been reported in popular venues, such as *Newsweek*, *Scientific American*, *The Economist*, *Smithsonian Magazine*, and the PBS documentary program *NOVA*. He is a Fellow of ASME.

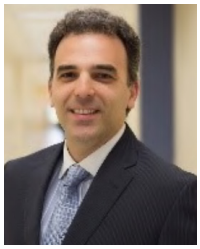

STAVROS V. GEORGAKOPOULOS (Senior Member, IEEE) received the Diploma degree in electrical engineering from the University of Patras, Patras, Greece, in June 1996, and the M.S. degree in electrical engineering and the Ph.D. degree in electrical engineering from Arizona State University, Tempe, AZ, USA, in 1998 and 2001, respectively. From 2001 to 2007, he was the Principal Engineer with SV Microwave, Inc. Since 2007, he has been with the Department of Electrical and Computer Engineering, Florida International University, Miami, FL, USA, where he is currently a Professor, the Director of Transforming Antennas Center (a research center on foldable/origami, physically reconfigurable and deployable antennas), and the Director of the RF Communications, Millimeter-Waves, and Terahertz Lab. His current research interests relate to novel antennas, arrays, RFID, microwave and RF systems, novel sensors and wireless powering of portable, as well as wearable and implantable devices. He received the 2015 FIU President's Council Worlds Ahead Faculty Award, which is the highest honor FIU extends to a faculty member for excelling in research, teaching, mentorship, and service. He served as an Associate Editor of the IEEE TRANSACTIONS ON ANTENNAS AND PROPAGATION from 2013 to 2019, and the IEEE OPEN JOURNAL OF ANTENNAS AND PROPAGATION since 2019.